Published in final edited form as:
J Neurochem. 2009 June ; 109(5): 1497–1507. doi:10.1111/j.1471-4159.2009.06078.x.

METABOTROPIC GLUTAMATE TYPE 5, DOPAMINE D_2 AND ADENOSINE A_{2A} RECEPTORS FORM HIGHER-ORDER OLIGOMERS IN LIVING CELLS

Nuria Cabello[1], **Jorge Gandía**[2], **Daniela C. G. Bertarelli**[1], **Masahiko Watanabe**[3], **Carme Lluís**[1], **Rafael Franco**[1], **Sergi Ferré**[4], **Rafael Luján**[5], and **Francisco Ciruela**[2]

[1] IDIBAPS, CIBERNED and Departament de Bioquímica i Biologia Molecular, Facultat de Biologia, Universitat de Barcelona, 08028 Barcelona, Spain

[2] Unitat de Farmacologia, Departament Patologia i Terapèutica Experimental, Facultat de Medicina, Universitat de Barcelona, L'Hospitalet de Llobregat, 08907 Barcelona, Spain

[3] Department of Anatomy, Hokkaido University, School of Medicine, Sapporo, Japan

[4] Behavioral Neuroscience Branch, National Institute on Drug Abuse, Intramural Research Program, National Institutes of Health, Department of Health and Human Services, Baltimore, MD 21224, USA

[5] Departamento de Ciencias Medicas, Facultad de Medicina-CRIB, Universidad de Castilla-La Mancha, Albacete, Spain

Abstract

G protein-coupled receptors are known to form homo- and heteromers at the plasma membrane, but the stoichiometry of these receptor oligomers are relatively unknown. Here, by using bimolecular fluorescence complementation, we visualized for the first time the occurrence of heterodimers of metabotropic glutamate $mGlu_5$ receptors ($mGlu_5R$) and dopamine D_2 receptors (D_2R) in living cells. Furthermore, the combination of bimolecular fluorescence complementation and bioluminescence resonance energy transfer techniques, as well as the sequential resonance energy transfer (SRET) technique, allowed us to detect the occurrence receptor oligomers containing more than two protomers, $mGlu_5R$, D_2R and adenosine A_{2A} receptor ($A_{2A}R$). Interestingly, by using high-resolution immunoelectron microscopy we could confirm that the three receptors co-distribute within the extrasynaptic plasma membrane of the same dendritic spines of asymmetrical, putative glutamatergic, striatal synapses. Also, co-immunoprecipitation experiments in native tissue demonstrated the existence of an association of $mGlu_5R$, D_2R and $A_{2A}R$ in rat striatum homogenates. Overall, these results provide new insights into the molecular composition of G protein-coupled receptor oligomers in general and the $mGlu_5R/D_2R/A_{2A}R$ oligomer in particular, a receptor oligomer that might constitute an important target for the treatment of some neuropsychiatric disorders.

Keywords

G protein-coupled receptors; adenosine; dopamine; glutamate; receptor oligomerization

Corresponding author: Francisco Ciruela, Unitat de Farmacologia, Dept. de Patologia i Terapèutica Experimental, Facultat de Medicina (Campus de Bellvitge), Pavelló de Govern, Av. Feixa Llarga, s/n, 08907 L'Hospitalet del Llobregat, Barcelona, Spain, Tel: +34-934024280/+34-934035820, Fax: +34-934029082, E-mail: fciruela@ub.edu.

Introduction

The striatum receives the densest dopamine innervation and contains the highest concentration of dopamine receptors in the brain (Gerfen, 2004; Lindvall and Bjorklund, 1978). As a consequence, dopamine plays a key role in motor activity and goal-directed behaviors and also in the pathophysiology of diverse disorders, including Parkinson's disease and drug addiction (Ferre *et al.*, 2004). Dopamine acts on G-protein-coupled receptors (GPCRs) that, based on sequence homologies and pharmacological profiles, have been classified in D_1-like, which include D_1 and D_5 receptors, and D_2-like receptors, which comprise the long and short isoforms of the D_2 receptor (termed D_{2L} and D_{2S}, respectively), the D_3 and the D_4 receptors (Missale *et al.*, 1998). The striatum also receives a dense glutamatergic innervation from cortical, thalamic and limbic areas (Gerfen, 2004). Several classes of glutamate receptors, widely distributed in the CNS, have been characterized: three subtypes of ionotropic glutamate (iGlu) receptors and a family of GPCRs, called metabotropic glutamate (mGlu) receptors, which act through different second messenger pathways. Eight members of the mGlu receptors family have been identified and categorized into three subgroups on the basis of their sequence homology, agonist selectivity and signal transduction pathway. Group I contains $mGlu_1$ and $mGlu_5$ receptor subtypes, which are coupled to phospholipase C in transfected cells and have quisqualic acid (Quis) as the most potent agonist.

In addition to dopamine and glutamate, adenosine plays a key role in basal ganglia function (Ferre *et al.*, 1997). Adenosine seems to be mainly produced by metabolism of ATP co-released with glutamate from nerve terminals and astrocytes (Ferre *et al.*, 2007) and mediates its actions by specific GPCRs, which are currently classified in A_1, A_{2A}, A_{2B}, and A_3 subtypes (Fredholm *et al.*, 2001). Compared to the other adenosine receptor subtypes, A_{2A} receptors (A_{2A}Rs) are particularly concentrated in the striatum (Ferre *et al.*, 1997; Rosin *et al.*, 1998), where they are mostly expressed by γ-aminobutyric acid (GABA)ergic striatopallidal neurons (Schiffmann *et al.*, 1991; Schiffmann *et al.*, 2007). Interestingly, ultrastructural analysis has demonstrated that A_{2A}Rs are localized mostly postsynaptically in the dendrites and dendritic spines of striatal GABAergic neurons (Hettinger *et al.*, 2001). A_{2A}R immunoreactivity was observed primarily at glutamatergic (asymmetric) synapses, predominantly at the postsynaptic but also at the presynaptic site (Ciruela *et al.*, 2006a; Hettinger *et al.*, 2001). Therefore, it has been suggested that A_{2A}R plays a key role in the fine-tuning modulation of glutamatergic neurotransmission in striatal GABAergic neurons both at the postsynaptic and presynaptic level (Ciruela *et al.*, 2006a; Ciruela *et al.*, 2006b; Ferre *et al.*, 2007; Ferre *et al.*, 2007; Hettinger *et al.*, 2001).

In the GABAergic striatopallidal neurons A_{2A}R are co-localized with D_2 receptors (D_2R), and establish functional A_{2A}R-D_2R heteromers (Ferre *et al.*, 2007; Ferre *et al.*, 2007) and, in the striatopallidal complex in primates, $mGlu_5$ receptor ($mGlu_5$R) showed a very similar localization to that described for A_{2A}R and D_2R in rats (Paquet and Smith, 2003). Furthermore, evidence has been provided for the existence of A_{2A}R-$mGlu_5$R heteromerization in transfected cells and in rat striatum (Ferre *et al.*, 2002). Significantly, multiple interactions between striatal A_{2A}R, D_2R and $mGlu_5$R were described at the biochemical and behavioural level (Ferre *et al.*, 2007; Ferre *et al.*, 2007; Ferre *et al.*, 2008; Fuxe *et al.*, 2003; Popoli *et al.*, 2001), suggesting the possible existence of higher-order $mGlu_5$R-D_2R-A_{2A}R oligomers. In the present study, for the first time, we provide evidence for the existence of $mGlu_5$R/D_2R/A_{2A}R oligomers in HEK-293 cells by two different experimental approaches, namely the combined use of bimolecular fluorescence complementation (BiFC) and bioluminescence energy transfer (BRET) (Gandia *et al.*, 2008a) and by sequential resonance energy transfer (SRET) (Carriba *et al.*, 2008). The

existence of these higher-order receptor oligomeric complexes might be relevant to striatal function both in normal and pathological conditions (Ferre *et al.*, 2003).

Materials and methods

Plasmid constructs

The cDNA encoding the $mGlu_{5b}$ receptor was subcloned into the *Eco*RI/*Bam*HI sites of $pGFP^2$-N3 (Perkin-Elmer, Waltham, MA, USA) and pEYFP-N1 (Clontech, Mountain View, CA, USA) vector as previously described (Cabello *et al.*, 2007). Also, the cDNA encoding dopamine D_2 receptor was amplified by PCR using the following primers: FD2Nhe (5′-CCGCGCTAGCATGGATCCACTGAATCTGTCC-3′) and RD2Xho (5′-CCGCTCGAGCCGCAGTGGAGGATCTTCAGG -3′) and cloned into the *Nhe*I/*Xho*I sites of p*R*luc-N1 vector (Perkin-Elmer). The other constructs used were previously described (Canals *et al.*, 2003). For the bimolecular complementation experiments a C-terminal truncated version of YFP, named N-YFP (amino acids 1 to 155), was made by PCR amplification and cloning into the *Xho*I site of pcDNA3.1 using the following primers: FnYFP (5′-CCGCTCGAGACCATGGTGAGCAAGGGCGAGGAGC-3′) and RnYFP (5′-CCGTCTAGATCAGGCCATGATATAGACGTTG-3′). Also, an N-terminal truncated version of YFP, named C-YFP (amino acids 155 to 231), was made using the same strategy and using the following primers: FcYFP (5′-CCGCTCGAGACCATGGACAAGCAGAAGAACGGC-3′) and RcYFP (5′-CCGTCTAGATTACTTGTACAGCTCGTCCAT-3′). The cDNAs encoding the D_2R, $mGlu_{5b}R$, $GABA_{B1b}R$ and $GABA_{B2}R$ without their stop codon were subcloned into the *Nhe*I/*Eco*RI or *Kpn*I/*Eco*RI sites of pcDNA3.1 vector (Invitrogen, Carlsbad, CA, U.S.A.), thus containing in frame the sequences for N-YFP or C-YFP. Finally, the cDNA encoding $A_{2A}R$ and $GABA_{B2}R$ without their stop codon were amplified using sense and antisense primers harboring unique restriction enzyme sites and subcloned to be in-frame with *R*luc in the p*R*luc-N1 vector or with EYFP in the pEYFP-N1 vector. Finally, besides the YFP constructs contained the ATG initiation codon when these were compared to the same constructs lacking the initiation codon neither apparent difference in molecular size nor in the subcellular distribution was observed, thus suggesting that no apparent translation took place from this second initiation codon (data not shown).

Antibodies

The primary antibodies used were: rabbit anti-$A_{2A}R$ whole serum (Ciruela *et al.*, 2004), rabbit anti-$A_{2A}R$ polyclonal antibody (Alomone Labs, Jerusalem, Israel), mouse anti-$A_{2A}R$ monoclonal antibody (clone 7F6-G5-A2; Millipore, Billerica, MA, USA), rabbit anti-D_2R whole serum (Bjelke *et al.*, 1996; Canals *et al.*, 2003; Jansson *et al.*, 1999; Levey *et al.*, 1993), rabbit anti-D_2R polyclonal antibody (Millipore), goat anti-D_2R polyclonal antibody (Santa Cruz, CA, USA), rabbit anti-D_2R polyclonal antibody (Narushima *et al.*, 2006), rabbit anti-$mGlu_5R$ polyclonal antibody (Millipore), guinea pig anti-$mGlu_5R$ polyclonal antibody (Uchigashima *et al.*, 2007b), mouse anti-GFP monoclonal antibody (Sigma-Aldrich, St. Louis, MO, USA). The secondary antibodies were: horseradish-peroxidase (HRP)-conjugated goat anti-rabbit IgG (Pierce, Rockford, IL, U.S.A.), HRP-conjugated rabbit anti-mouse IgG (Dako, Denmark), HRP-conjugated anti-rabbit IgG TrueBlot (eBioscience, San Diego, CA, USA), donkey anti-rabbit-Cy5™ (Jackson ImmunoResearch Laboratories, Inc., West Grove, PA, USA), donkey anti-mouse-Cy3™ (Jackson ImmunoResearch Laboratories, Inc.), donkey anti-goat-Cy2™ (Jackson ImmunoResearch Laboratories, Inc.), goat anti-mouse IgG conjugated to 10 nm colloidal gold (1/100; Aurion, Wageningen, The Netherlands), goat anti-rabbit IgG conjugated to 15 nm colloidal gold (1/100; Aurion) and goat anti-guinea pig IgG conjugated to 20 nm colloidal gold (1/100; Aurion).

Cell culture, transfection and membrane preparation

Human embryonic kidney (HEK-293) cells were grown in Dulbecco's modified Eagle's medium, DMEM (Sigma-Aldrich) supplemented with 1 mM sodium pyruvate, 2 mM L-glutamine, 100 U/ml streptomycin, 100 μg/ml penicillin and 10% (v/v) foetal bovine serum (FBS) at 37°C and in an atmosphere of 5% CO2. HEK-293 cells growing in 25 cm^2 flasks or in 6-well plates, containing 20 mm coverslips when used for confocal microscopy, were transiently transfected with the DNA encoding the specified proteins by the calcium phosphate precipitation technique (Jordan *et al.*, 1996). The cells were harvested at either 24 or 48 hours after transfection. Membrane suspensions from transfected HEK-293 cells or from rat striatum were obtained as described previously (Burgueno *et al.*, 2003).

Immunoprecipitation and Immunostaining

For immunoprecipitation membranes from transiently transfected HEK cells or from rat striatum were solubilized in ice-cold RIPA buffer (50 mM Tris·HCl pH 7.4, 100 mM NaCl, 1% Triton-X100, 0.5% sodium deoxycholate, 0.2% SDS and 1 mM EDTA) for 30 min on ice. The solubilized preparation was then centrifuged at 13.000xg for 30 min. The supernatant (1mg/ml) was processed for immunoprecipitation, each step of which was conducted with constant rotation at 0–4 °C. The supernatant was incubated overnight with the indicated antibody. Then 40 μl of either a suspension of protein G cross linked to agarose beads or TrueBlot™ anti-Rabbit Ig IP Beads (eBioscience) were added and the mixture was incubated overnight. Subsequently, the beads were washed twice with ice-cold RIPA buffer, twice with ice cold RIPA buffer diluted 1:10 in TBS (50 mM Tris·HCl pH 7.4, 100 mM NaCl) and once with TBS and aspirated to dryness with a 28-gauge needle. Subsequently, 30μl of SDS-PAGE sample buffer (8M Urea, 2% SDS, 100mM DTT, 375mM Tris, pH 6.8) was added to each sample. Immune complexes were dissociated by heating to 37°C for 2 h and resolved by SDS-polyacrylamide gel electrophoresis in 6.5% or 10% gels and immunoblotted as described above.

For immunocytochemistry transiently transfected HEK-293 cells were fixed in 4% paraformaldehyde for 15 min, and washed with phosphate buffered saline (PBS) containing 20 mM glycine (buffer A) to quench the remaining free aldehyde groups. Cells were permeabilized with buffer A containing 0.2% Triton X-100 for 5 minutes. Blocking was done using buffer A containing 1% BSA (buffer B). Cells were labeled for 1 h at room temperature with the indicated primary antibody, washed for 30 min in buffer B and stained with the corresponding secondary antibodies for another hour. Samples were rinsed and observed in a confocal microscope (Lujan and Ciruela, 2001; Sarrio *et al.*, 2000).

For electron microscopy, ultrathin sections (70–90 nm) from three Lowicryl-embedded blocks were incubated for 45 min on pioloform-coated nickel grids with drops of blocking solution consisting of 2 % albumin in 0.05 M TBS, 0.9 % NaCl and 0.03 % Triton X-100. The grids were transferred to a mixture solution A2AR, D2R and mgluR5 antibodies at a final protein concentration of 10 μg/mL diluted in blocking solution overnight at room temperature. After several washes in TBS, grids were incubated for 2 h in drops of a mixture of goat anti-mouse IgG conjugated to 10 nm-colloidal gold particles, goat anti-rabbit IgG conjugated to 15 nm-colloidal gold particles and goat anti-guinea pig IgG conjugated to 20 nm-colloidal gold particles (Aurion, Wageningen, The Netherlands), each diluted 1:100 in a 0.05 M TBS solution containing 2 % normal human serum and 0.5 % polyethylene glycol. Grids were then washed in TBS for 30 min and counterstained for electron microscopy with saturated aqueous uranyl acetate and lead citrate. Ultrastructural analyses were performed in a Jeol-1010 electron microscope. Electron photomicrographs were captured with CCD camera (Mega View III; Soft Imaging System, Germany). Digitized electron images were

then modified for brightness and contrast by using Adobe PhotoShop CS1 (Mountain View, CA) to optimize them for printing.

Gel electrophoresis and immunoblotting

Sodium dodecyl sulfate polyacrylamide gel electrophoresis (SDS/PAGE) was performed using 7.5 or 10 % polyacrylamide gels. Proteins were transferred to PVDF membranes using a semi-dry transfer system and immunoblotted with the indicated antibody and then HRP-conjugated goat anti-rabbit IgG (1/30000), HRP-conjugated rabbit anti-mouse IgG (1/5000) or HRP-conjugated anti-rabbit IgG TrueBlot (1/1000). The immunoreactive bands were developed using a chemiluminescent detection kit (Pierce) (Ciruela and McIlhinney, 1997).

Resonance energy transfer-based methods

For bioluminescence resonance energy transfer (BRET) experiments HEK cells transiently transfected with a constant amount of cDNA encoding the D_2R^{Rluc} and increasing amounts of $A_{2A}R^{YFP}$ or CD_4R^{YFP} were detached, washed and resuspended in HBSS buffer containing 10 mM glucose. To maintain the same ratio of DNA in cotransfections, we used empty vector, pcDNA3.1, to equilibrate the amount of total DNA transfected. To control for cell number, protein concentration in the samples was determined using a Bradford assay kit (Bio-Rad, Hercules, CA, USA) using bovine serum albumin dilutions as standards. Cell suspension (20 μg protein) was distributed in duplicate into 96-well microplates (black plates with a transparent bottom for fluorescence measurement or white plates with white bottom for BRET determination). Fluorescence and bioluminescence readings were collected using a Mithras LB 940 (Berthold Technologies, DLReady, Germany) that allows the integration of the signals detected in the filter at 485 nm (440–500 nm, maximum in bioluminescence emission) and 530 nm (510–590 nm, maximum in YFP emission). YFP fluorescence was defined as the fluorescence of the sample minus the fluorescence of cells expressing only *R*luc-tagged receptor. For BRET measurement, 5 μM h-coelenterazine (Molecular Probes, Eugene, OR, USA) was added to the samples and readings were performed after 1 min (net BRET determination) and 10 min (*R*luc luminiscence quantification). BRET signal was determined by calculating the ratio of the light emitted by YFP (510–590 nm) over the light emitted by the *R*luc (440–500 nm). The net BRET values were obtained by subtracting the BRET background signal detected when *R*luc-tagged construct was expressed alone. Curves were fitted using nonlinear regression and one-phase exponential association fit equation (GraphPad Prism, San Diego, CA, USA).

Displacement studies were performed at a constant BRET ratio, around the $BRET_{50}$ of the $A_{2A}R^{Rluc}/D_2R^{YFP}$ pair, and increasing amounts of $mGlu_5R$ or CD_4R constructs. The BRET values were expressed as a percentage of the $BRET_{50}$ of the $mGlu_5R$ nontransfected cells and better fitted to a two site competition curve using nonlinear regression (GraphPad Prism). The combined BRET-bimolecular fluorescence complementation (BiFC) assay was performed as described recently (Gandia *et al.*, 2008a). Briefly, cells transfected with indicated plasmids were placed in DMEM medium for 24 hours at 37oC, followed by another 24 hours at 30oC in order to allow proper the maturation of complemented fluorophore (Schmidt *et al.*, 2006). After transfection cells were processed for BRET measurements as described above.

For Sequential Ressonance Energy Transfer (SRET) experiments HEK-293 cells were transiently co-transfected with plasmid encoding $D_{2L}R^{Rluc}$ (2 μg), $mGlu_5R^{GFP2}$ (4 μg) and $A_{2A}R^{YFP}$ (6 μg for a single SRET experiment or increasing amounts for SRET curves), as described previously (Carriba *et al.*, 2008). Fluorescence and luminescence were determined as described above. For SRET measurements cells were distributed in 96-white well microplates and 5 μM DeepBlueC (Molecular Probes) was added. SRET signal was

collected in a Mithras LB 940 using the detected filters at short-wavelength at 485 nm (440–500 nm) and at long-wavelength at 530 nm (510–590 nm). Here, we express net SRET as [(long-wavelength emission)/(short-wavelength emission)]-Cf where Cf corresponds to [(long-wavelength emission)/(short-wavelength emission)] for cells expressing $D_{2L}R^{Rluc}$, $mGlu_5R^{GFP2}$ (Carriba *et al.*, 2008). Curves were fitted as described above.

Results

Investigation of $mGlu_5R$, $A_{2A}R$ ad D_2R oligomerization by classical biochemical approaches

The association of the D_2R with $mGlu_5R$ and $A_{2A}R$ was first studied by classical biochemical approaches, namely immunolabeling experiments and coimmunoprecipitation assays. Thus, by means of confocal microscopy analysis of HEK-293 cells transiently transfected with the cDNAs encoding for the D_2R, $A_{2A}R$ and $mGlu_5R$ some overlapping in the distribution of the three receptors was found (Fig. 1a). Interestingly, it is important to mention here that around 70% of the cells were simultaneously expressing all three receptors. Next, the existence of $mGlu_5R/A_{2A}R/D_2R$ oligomers was subsequently assayed by co-immunoprecipitation experiments. From extracts of HEK-293 cells transfected with $mGlu_5R^{GFP2}$ (Fig. 1b, lane 1), D_2R (Fig. 1b, lane 2), $A_{2A}R$ (Fig. 1b, lane 3) or with $A_{2A}R$ plus D_2R plus $mGlu_5R^{GFP2}$ (Fig. 1b, lane 4) the mouse monoclonal antibody against GFP, which recognizes all GFP variants, immunoprecipitated a band of ~160 kDa, which corresponds to the $mGlu_5R^{GFP2}$ (Fig. 1b, IP: GFP, lanes 1 and 4, lower panel). This band did not appear in immunoprecipitates from cells transfected only with the cDNA encoding for D_2R (Fig. 1b, lane 2, lower panel) or $A_{2A}R$ (Fig. 1b, lane 3, lower panel) or when an irrelevant antibody was used (data not shown). Interestingly, when immunoprecipitates from the triple-transfected cells were analyzed by immunoblot using an antibody against the $A_{2A}R$, a band of ~42 kDa, which corresponds to the $A_{2A}R$, was observed (Fig. 1b, IP:GFP, lane 4, upper panel), and similarly, when these immunoprecipitates were analyze by western-blot using an antibody against the D_2R, a band of ~90 kDa, which corresponds to the D_2R, was observed (Fig. 1b, IP:GFP, lane 4, middle $_2$ panel). Importantly, similar results were obtained when $A_{2A}R$ and D_2R were tagged with GFP and analogous co-immunoprecipitation experiments were performed (Fig. 1c and d). Overall, these results suggest that $mGlu_5R$, $A_{2A}R$ and D_2R are expressed in the same membrane domain and might form receptor heteromers.

Study of $A_{2A}R/D_2R$, $mGlu_5R/A_{2A}R$ and $mGlu_5R/D_2R$ oligomers by BRET assays

Although the use of biochemical approaches to demonstrate receptor oligomerization has been widely used, it might have some disadvantages since the cellular structure is destroyed by detergent treatment. Thus, in order to assess if $mGlu_5R$, $A_{2A}R$ and D_2R form oligomers in living cells, biophysical approaches were performed in cells transiently transfected with receptor constructs that carry appropriate fluorophore pairs in their C-terminus. Initially, by using a BRET approach, a positive and saturable BRET signal for the transfer of energy between D_2R^{Rluc} and $A_{2A}R^{YFP}$ in cells co-transfected with a constant concentration of the $D_{2L}R^{Rluc}$ and increasing concentrations of $A_{2A}R^{YFP}$ was observed (Fig. 2a). As the control pair $D_{2L}R^{Rluc}$ and CD_4R^{YFP} led to a quasi-linear curve, the specificity of the saturation (hyperbolic) assay for the $D_{2L}R^{Rluc}$ and $A_{2A}R^{YFP}$ pair could be established (Fig. 2a). Similarly, $BRET^2$ studies between $A_{2A}R^{Rluc}$ and $mGlu_5R^{GFP2}$ and between $D_{2L}R^{Rluc}$ and $mGlu_5R^{GFP2}$ were performed and similar results obtained (data not shown). These results clearly corroborate previous studies about heterodimerization of $A_{2A}R$ with D_2R and $A_{2A}R$ with D_2R (Canals *et al.*, 2003; Ciruela *et al.*, 2004; Ferre *et al.*, 2002), and demonstrate the ability of D_2R to heteromerize with $mGlu_5R$. Interestingly, when the adenosine A_1 receptor (A_1R) and the $GABA_{B2}$ receptor ($GABA_{B2}R$) were used as acceptors molecules (e.g.

A_1R^{YFP} and $GABA_{B2}R^{YFP}$) in a BRET process with the $D_{2L}R^{Rluc}$ a considerable lower BRET efficiency was observed (Fig. 2b). These results suggest that receptors with none predicted physiological heteromer complex formation with $D_{2L}R$ (e.g. A_1R and $GABA_{B2}R$) might indeed be used as negative controls in BRET experiments.

To initially test the ability of these receptors to form heterotrimers, we performed a set of BRET competition experiments. Thus, HEK-293 were transiently transfected with a constant ratioof $A_{2A}R^{Rluc}$ and D_2R^{YFP} (2μg and 1μg, respectively), that was around the $BRET_{50}$ of this BRET pair, and increasing amounts of $mGlu_5R$ or CD_4R (Fig. 2c). As shown in Fig. 2b, under these conditions $mGlu_5R$ was able to reduce the $BRET_{50}$ efficiency of the $A_{2A}R^{Rluc}/D_2R^{YFP}$- BRET pair in a biphasic mode. Conversely, increasing amounts of $A_{2A}R$ were able to reduce $BRET_{50}$ efficiency of the $D_2R^{Rluc}/mGlu_5R^{YFP}$-BRET pair in a biphasic fashion (Fig. 2c). It is important to mention here that co-transfection of a fixed amount of the $A_{2A}R^{Rluc}/mGlu_5R^{YFP}$-BRET pair with increasing amounts of D_2R produced a markedly alteration of the donor/acceptor (e.g. $A_{2A}R\ _R{}^{luc}/mGlu_5R^{YFP}$) ratio, thus precluding BRET efficiencies comparison (data not shown). Finally, no competition of CD_4R with the $A_{2A}R^{Rluc}/D_2R^{YFP}$-BRET pair was observed (Fig. 2c). Overall, these results suggest that both $mGlu_5R$ and $A_{2A}R$ can either compete for the same D_2R binding site with two different affinities or two different binding sites with different affinities exists within the D_2R structure.

A combined BRET/BiFC assay to determine the existence of higher-order $mGlu_5R/A_{2A}R/D_2R$ oligomers

As shown above, the existence of $mGlu_5R/A_{2A}R/D_2R$ oligomers can be indirectly shown by using a combination of biochemical and biophysical techniques, but these approaches do not directly prove the existence of receptor complexes containing more than two protomers. For that purpose, we used a new experimental approach recently described (Gandia *et al.*, 2008a) which consists in the combination of BRET and BiFC techniques (Fig. 3a). The BiFC assay, a protein fragment complementation method (Kerppola, 2006a), is based on the ability to produce a fluorescent complex from non-fluorescent constituents if a protein-protein interaction occurs (Kerppola, 2006b). To this end, $mGlu_5R$ and D_2R fused at the C terminal with N-YFP and C-YFP fragments were generated and transfected into HEK cells. Cells single transfected with receptors containing either the C-YFP or N-YFP fragments in their C-terminal tail did not provide a positive fluorescent signal, (data not shown). Since receptor heterodimerization caused YFP reconstitution, thus allowing fluorescence detection, we were able to visualize $mGlu_5R/D_2R$ heterodimers in living cells (Fig. 3b). On the other hand, it has been previously shown that fluorescent protein fragments are able to complement with low efficiency, thus forming fluorescent complexes, even in the absence of a specific interaction (Kerppola, 2006b). Therefore, some control experiments were designed to ensure that receptor heterodimerization was not driven by spontaneous YFP complementation. The most appropriate negative controls for this technique are fusion proteins that are expressed in the same subcellular compartment than the proteins under study but that are not able to interact. In this study we have used other unrelated GPCRs as negative controls, namely the $GABA_{B1b}R$ and $GABA_{B2}R$. Under the same experimental conditions, we were not able to detect fluorescence complementation between the $mGlu_5R$ or D_2R and either the $GABA_{B1b}R$ or $GABA_{B2}R$ (data not shown). Overall, these results convincingly show for the first time that $mGlu_5R$ and D_2R do heterodimerize and that the $mGlu_5R/D_2R$ heterodimers are located at the plasma membrane level of living cells (Fig. 3b, right panel)

Under the same experimental conditions, we performed a BRET saturation curve in cells co-transfected with a constant amount of the $A_{2A}R^{Rluc}$ construct and increasing concentrations

of the $mGlu_5R^{N\text{-}YFP}$+$D_2R^{C\text{-}YFP}$ plasmids or $GABA_{B2}R^{YFP}$. A positive BRET signal for the transfer of energy between $A_{2A}R^{Rluc}$ and $mGlu_5R^{N\text{-}YFP}$ +$D_2R^{C\text{-}YFP}$ was obtained (Fig. 3c). The BRET signal increased as a hyperbolic function of the heterodimer-mediated complemented YFP (assessed by the fluorescence emitted upon direct excitation at 480 nm), thus strongly suggesting the formation of receptor oligomers containing more than two protomers, i.e. $mGlu_5R/D_2R/A_{2A}R$ oligomers (Fig. 3c).

SRET in the study of higher-order $mGlu_5R/A_{2A}R/D_2R$ oligomers

To pursue the direct detection of $mGlu_5R/D_2R/A_{2A}R$ oligomer formation, we implemented a new experimental approach developed by our research group (Carriba *et al.*, 2008). This technique, named SRET, engage a $BRET^2$ method with a FRET process (Carriba *et al.*, 2008) (Fig. 4a). SRET is based on an adequate combination of donors and acceptors for BRET and for FRET and on the fact that different emission profiles result from the use of different *R*luc substrates. Thus, DeepBlueC is used as a trigger agent for SRET instead of coelenterazine H. By the action of *R*luc, oxidation of DeepBlueC is able to excite GFP^2, which is a so called $BRET^2$ signal. While returning to the ground state, excited GFP^2 emits energy that excites YFP, providing a FRET signal. For a specified level of expression of the receptor coupled to the luciferase (*R*luc), the highest SRET efficiency is observed when the FRET donor is relatively low whereas the expression of the FRET acceptor is relatively high. Therefore, we performed a set of preliminary experiments to establish the optimal concentrations of receptor constructs that need to be transfected to provide a maximum $BRET^2$ and FRET efficiency with the minimum photophysic cross-talks (Supplementary Fig. 1) (Carriba *et al.*, 2008; Ciruela, 2008). Once the optimal conditions were found, we performed a single SRET measurement to characterize the $mGlu_5R/D_2R/A_{2A}R$ oligomer. Thus, by using the following fusion protein ratio: $D_{2L}R^{Rluc}$ (2 μg), $mGlu_5R^{GFP2}$ (4μg) and $A_{2A}R^{YFP}$ (8 μg), we obtained a positive and specific SRET signal (Fig. 4b). Next, we performed a SRET saturation curve. Thus, HEK-293 cells co-expressing a constant ratio of $D_{2L}R^{Rluc}$(2 μg) plus $mGlu_5R^{GFP2}$(4 μg) and increasing amounts of $A_{2A}R^{YFP}$ or CD_4R^{YFP} (Fig. 4c). Again, we could establish the specificity of the $mGlu_5R/D_2R/A_{2A}R$ oligomer formation, since we obtained a saturable (hyperbolic) curve when compared to the negative control (Fig. 4c)

$mGlu_5R/D_2R/A_{2A}R$ interactions in rat striatum

The demonstration of $mGlu_5R/D_2R/A_{2A}R$ oligomers in living cells provides for a morphological framework for the already known multiple functional interactions between these receptors in the brain (see Introduction). To asses the physiological significance of the $mGlu_5R/D_2R/A_{2A}R$ interaction co-immunoprecipitation experiments were performed using rat striatum homogenates. Using soluble extracts from rat striatum the anti-$A_{2A}R$ antibody was able to immunoprecipitate a band around 45 kDa which corresponds to the striatal $A_{2A}R$, as expected (Fig. 5a). Interestingly, this antibody was able to immunoprecipitate the D_2R (~90 kDa) and $mGlu_5R$ (~130 kDa) from the same extracts (Fig. 5a, lane 2). These bands did not appear when an irrelevant rabbit IgG was used for immunoprecipitation (Fig. 5a, lane 1), showing that the reaction was specific. Conversely, the anti-D_2R antibody was able to immunoprecipitate the $A_{2A}R$ and $mGlu_5R$ and the anti-$mGlu_5R$ antibody the $A_{2A}R$ and D_2R, respectively (Fig. 5a). Overall, these results suggest that $mGlu_5R$, D_2R and $A_{2A}R$ do oligomerize in native tissue, namely striatum, and that this oligomerization might be physiologically relevant.

To provide the precise morphological evidence and to elucidate the subcellular localization of the $mGlu_5R/D_2R/A_{2A}R$ oligomer in neurons of the rat striatum, we performed triple-labelling post-embedding immunogold techniques at electron microscopic level. Thus, we have showed here that $mGlu_5R$, D_2R and $A_{2A}R$ co-distributed in postsynaptic structures

along the extra-synaptic and peri-synaptic plasma membrane of spines, establishing asymmetrical, putative glutamatergic, synapses with axon terminals (Fig. 5b). This precise distribution of $mGlu_5R$, D_2R and $A_{2A}R$ in striatal neurons resembles that previously described for these receptors (Uchigashima *et al.*, 2007a)(Ciruela *et al.*, 2006a). Overall, this is the first direct anatomic evidence for $mGlu_5R$, D_2R and $A_{2A}R$ co-distribution in the same neuronal compartment and support the idea that the $mGlu_5R/D_2R/A_{2A}R$ oligomer localized in the GABAergic striatopallidal neurons might play a key role in striatal function both in normal and pathological conditions.

Discussion

A key aim of post-genomic biomedical research is to systematically catalogue all molecules and their interactions in a living cell. Many fundamental cellular processes involve multiple interactions among proteins and other biomolecules, i.e. biomolecular interaction networks (Xia *et al.*, 2004). Protein-protein physical interactions constitute an important group of biomolecular interaction networks (Xia *et al.*, 2004), such as the neuronal horizontal molecular networks (Agnati *et al.*, 2003; Bockaert *et al.*, 2003; Franco *et al.*, 2003). Horizontal molecular networks take place at the neuronal plasma membrane level, where specific GPCR interact and integrate the messages provided by a variety of neurotransmitters. Immunodetection and co-immunoprecipitation assays are being used successfully to draw a map of molecular networks involving protein-protein interactions of cytosolic proteins. In contrast, these techniques have limitations when analyzing heptaspanning membrane receptors. In the early eighties, and based on indirect functional evidences, it was proposed that GPCR receptors could interact at the level of the neuronal plasma membrane. In the early nineties, electrophoretic mobility and co-immunoprecipitation assays gave the first indication of GPCR homomerization. More recently, several experimental approaches have been used in the study of the quaternary structure of GPCRs, revealing the existence of receptor homo- and heteromers (Milligan and Bouvier, 2005). Among these approaches, fluorescence-based methods, as non-invasive techniques, have played a key role in the characterization of a large array of protein-protein interactions in general and in the study of GPCR oligomerization in particular (Gandia *et al.*, 2008b). The use of the biophysical techniques BRET and FRET, allowed the demonstration of GPCR homodimerization and heterodimerization GPCRs in living cells (Agnati *et al.*, 2003; Bouvier, 2001; Franco *et al.*, 2003). We and others have recently introduced a set of new techniques based on the combination of RET-based methods together with Bimolecular Fuorescence/Luminescence Complementation techniques (BiFC and BiLC, respectively) that has made possible to detect GPCR heteromers constituted by more than two receptors (Carriba *et al.*, 2008; Dupre *et al.*, 2006; Gandia *et al.*, 2008a; Guo *et al.*, 2008; Lopez-Gimenez *et al.*, 2007; Navarro *et al.*, 2008; Vidi *et al.*, 2008).

The existence of functional $mGlu_5R/D_2R/A_{2A}R$ oligomers in the GABAergic striatopallidal neuron has often been discussed in the literature, based on the high and selective co-expression of $mGlu_5R$, D_2R and $A_{2A}R$ in these particular cells (see Introduction), on the demonstration of $A_{2A}R/D_2R$ and $A_{2A}R/mGlu_5R$ heteromers (see Introduction) and on the existence of strong multiple interactions between the three receptors (see below). However, the demonstration of their simultaneous physical interaction had not yet been reported. By using immunodetection and co-immunoprecipitation, BRET competition, BRET/BiFc and SRET techniques, this study provides clear evidence for the existence of the $mGlu_5R/D_2R/A_{2A}R$ oligomers in living cells and in rat striatum. Co-immunodetection and co-immunoprecipitation experiments demonstrated that when co-expressed in the same cell or in native tisue, $mGlu_5R$, D_2R and $A_{2A}R$ are physically linked in the cell membrane. BRET competition experiments gave indirect evidence for the existence of $mGlu_5R/D_2R/A_{2A}R$ oligomers, by demonstrating that co-expression of $mGlu_5R$ significantly modified the BRET

signal of the heteromer formed by $A_{2A}R^{Rluc}$ and D_2R^{YFP}. Also, the direct proof for $mGlu_5R/D_2R/A_{2A}R$ oligomerization came from experiments with BRET/BiFC and SRET. Finally, our immunogold experiments clearly demonstrated the specific postsynactic location of the $mGlu_5R/D_2R/A_{2A}R$ oligomer in GABAergic striatopallidal neurons. However, it is important to mention here that apart of the assumed postsynaptic interaction describe here a putative presynaptic interaction for $A_{2A}R/mGlu_5R$ and $A_{2A}R/D_2R$ has been also showed (Rodrigues *et al.*, 2005; Tozzi *et al.*, 2007). To this regard we can not exclude the possibility that the $mGlu_5R/D_2R/A_{2A}R$ oligomer might also exists presynaptically, thus controlling the excitability and firing of medium spiny neurons. This is an issue that deserves more future work.

Strong functional antagonistic interactions between $A_{2A}R$ and D_2R were first described and recently reviewed (Ferre *et al.*, 2008)) and, later on, antagonistic interactions between $mGlu_5R$ and D_2R and synergistic interactions between $A_{2A}R$ and $mGlu_5R$ were also reported (Ferre *et al.*, 2002; Popoli *et al.*, 2001). In membrane preparations from rat striatum, stimulation of either $A_{2A}R$ or $mGlu_5R$ produces a decrease in the affinity of D_2R for agonists and a decrease in D_2R agonist-mediated motor activation (Ferre *et al.*, 1991; Popoli *et al.*, 2001). Interestingly, co-stimulation of $A_{2A}R$ and $mGlu_5R$ produces a synergistic antagonistic modulation of D_2R ligand binding and function that is significantly stronger than the reduction induced by stimulation of either receptor alone (Popoli *et al.*, 2001). Thus, co-administration of $A_{2A}R$ and $mGlu_5R$ agonists inhibits motor activation induced by D_2R agonists (Ferre *et al.*, 2002; Popoli *et al.*, 2001). Also, central $A_{2A}R$ and $mGlu_5R$ agonist co-administration counteracts the inhibitory effect that endogenous dopamine exerts on *c-fos* expression by tonically stimulating striatal D_2R (Ferre *et al.*, 2002). It was, therefore, hypothesized that the multiple $mGlu_5R$-D_2R-$A_{2A}R$ interactions could provide a new therapeutic approach for some neuropsychiatric disorders, such as Parkinson's disease (Fuxe *et al.*, 2003; Popoli *et al.*, 2001). In fact, $A_{2A}R$ antagonists are being shown to be clinically useful as antiparkinsonian agents (Muller and Ferre, 2007). Also, there is preclinical evidence for the efficacy of $mGlu_5R$ antagonists (Ossowska *et al.*, 2001)(Breysse *et al.*, 2002) and, more importantly, for a synergistic effect of $A_{2A}R$ and $mGlu_5R$ antagonists in animal models of Parkinson's disease (Coccurello *et al.*, 2004; Kachroo *et al.*, 2005). Hyperactivity of the GABAergic striatopallidal neuron is a main pathophysiological mechanism responsible for hypokinesia in Parkinson's disease (Obeso *et al.*, 2000). The reported synergistic antiparkinsonian effect of $A_{2A}R$ and $mGlu_5R$ antagonists in animal models (Coccurello *et al.*, 2004; Kachroo *et al.*, 2005) suggests that the dopamine depletion-induced hyperactivity of striatopallidal neurons depends on a synergistic stimulatory endogenous tone of endogenous adenosine and glutamate on $A_{2A}R$ and $mGlu_5R$, upon interruption of D_2R signaling.

In summary, in the present study we provide biochemical evidence that supports the existence of $mGlu_5R$-D_2R-$A_{2A}R$ heteromers in living cells and strongly suggest their presence in the brain, in the GABAergic striatopallidal neurons, where they can provide important targets for the treatment of neuropsychiatric disorders.

Acknowledgments

This work was supported by grants SAF2008-01462 and Consolider-Ingenio CSD2008-00005 from Ministerio de Ciencia e Innovacion and by Sociedad Espanola de Farmacologia and Almirall Prodesfarma to FC. Also, supported by the Junta de Comunidades de Castilla-La Mancha (PAI08-0174-6967) to RL and by the Intramural funds of the National Institute on Drug Abuse, NIH.

References

Agnati LF, Ferre S, Lluis C, Franco R, Fuxe K. Molecular mechanisms and therapeutical implications of intramembrane receptor/receptor interactions among heptahelical receptors with examples from the striatopallidal GABA neurons. Pharmacol Rev. 2003; 55:509–550. [PubMed: 12869660]

Bjelke B, Goldstein M, Tinner B, et al. Dopaminergic transmission in the rat retina: evidence for volume transmission. J Chem Neuroanat. 1996; 12:37–50. [PubMed: 9001947]

Bockaert J, Marin P, Dumuis A, Fagni L. The 'magic tail' of G protein-coupled receptors: an anchorage for functional protein networks. FEBS Lett. 2003; 546:65–72. [PubMed: 12829238]

Bouvier M. Oligomerization of G-protein-coupled transmitter receptors. Nat Rev Neurosci. 2001; 2:274–286. [PubMed: 11283750]

Breysse N, Baunez C, Spooren W, Gasparini F, Amalric M. Chronic but not acute treatment with a metabotropic glutamate 5 receptor antagonist reverses the akinetic deficits in a rat model of parkinsonism. J Neurosci. 2002; 22:5669–5678. [PubMed: 12097518]

Burgueno J, Enrich C, Canela EI, Mallol J, Lluis C, Franco R, Ciruela F. Metabotropic glutamate type 1alpha receptor localizes in low-density caveolin-rich plasma membrane fractions. J Neurochem. 2003; 86:785–791. [PubMed: 12887677]

Cabello N, Remelli R, Canela L, et al. Actin-binding protein alpha-actinin-1 interacts with the metabotropic glutamate receptor type 5b and modulates the cell surface expression and function of the receptor. J Biol Chem. 2007; 282:12143–12153. [PubMed: 17311919]

Canals M, Marcellino D, Fanelli F, et al. Adenosine A2A-dopamine D2 receptor-receptor heteromerization: qualitative and quantitative assessment by fluorescence and bioluminescence energy transfer. J Biol Chem. 2003; 278:46741–46749. [PubMed: 12933819]

Carriba P, Navarro G, Ciruela F, et al. Detection of heteromerization of more than two proteins by sequential BRET-FRET. Nat Methods. 2008; 5:727–733. [PubMed: 18587404]

Ciruela F. Fluorescence-based methods in the study of protein-protein interactions in living cells. Curr Opin Biotechnol. 2008

Ciruela F, Burgueno J, Casado V, et al. Combining mass spectrometry and pull-down techniques for the study of receptor heteromerization. Direct epitope-epitope electrostatic interactions between adenosine A2A and dopamine D2 receptors. Anal Chem. 2004; 76:5354–5363. [PubMed: 15362892]

Ciruela F, Casado V, Rodrigues RJ, et al. Presynaptic control of striatal glutamatergic neurotransmission by adenosine A1-A2A receptor heteromers. J Neurosci. 2006a; 26:2080–2087. [PubMed: 16481441]

Ciruela F, Ferre S, Casado V, Cortes A, Cunha RA, Lluis C, Franco R. Heterodimeric adenosine receptors: a device to regulate neurotransmitter release. Cell Mol Life Sci. 2006b; 63:2427–2431. [PubMed: 17058035]

Ciruela F, McIlhinney RA. Differential internalisation of mGluR1 splice variants in response to agonist and phorbol esters in permanently transfected BHK cells. FEBS Lett. 1997; 418:83–86. [PubMed: 9414100]

Coccurello R, Breysse N, Amalric M. Simultaneous blockade of adenosine A2A and metabotropic glutamate mGlu5 receptors increase their efficacy in reversing Parkinsonian deficits in rats. Neuropsychopharmacology. 2004; 29:1451–1461. [PubMed: 15039773]

Dupre DJ, Robitaille M, Ethier N, Villeneuve LR, Mamarbachi AM, Hebert TE. Seven transmembrane receptor core signaling complexes are assembled prior to plasma membrane trafficking. J Biol Chem. 2006; 281:34561–34573. [PubMed: 16959776]

Ferré S, Ciruela F, Woods A, et al. Glutamate $mGluR_5$/adenosine A_{2A}/dopamine D_2 receptor interactions in the striatum. Implications for drug therapy in neuro-psychiatric disorders and drug abuse. Curr Med Chem -Cen Nerv Sys Ag. 2003; 3:1–26.

Ferre S, Agnati LF, Ciruela F, Lluis C, Woods AS, Fuxe K, Franco R. Neurotransmitter receptor heteromers and their integrative role in 'local modules': the striatal spine module. Brain Res Rev. 2007; 55:55–67. [PubMed: 17408563]

Ferre S, Ciruela F, Canals M, et al. Adenosine A2A-dopamine D2 receptor-receptor heteromers. Targets for neuro-psychiatric disorders. Parkinsonism Relat Disord. 2004; 10:265–271. [PubMed: 15196504]

Ferre S, Ciruela F, Woods AS, Lluis C, Franco R. Functional relevance of neurotransmitter receptor heteromers in the central nervous system. Trends Neurosci. 2007; 30:440–446. [PubMed: 17692396]

Ferre S, Fredholm BB, Morelli M, Popoli P, Fuxe K. Adenosine-dopamine receptor-receptor interactions as an integrative mechanism in the basal ganglia. Trends Neurosci. 1997; 20:482–487. [PubMed: 9347617]

Ferre S, Karcz-Kubicha M, Hope BT, et al. Synergistic interaction between adenosine A2A and glutamate mGlu5 receptors: implications for striatal neuronal function. Proc Natl Acad Sci U S A. 2002; 99:11940–11945. [PubMed: 12189203]

Ferre S, Quiroz C, Woods AS, Cunha R, Popoli P, Ciruela F, Lluis C, Franco R, Azdad K, Schiffmann SN. An update on adenosine A2A-dopamine D2 receptor interactions: implications for the function of G protein-coupled receptors. Curr Pharm Des. 2008; 14:1468–1474. [PubMed: 18537670]

Ferre S, von Euler G, Johansson B, Fredholm BB, Fuxe K. Stimulation of high-affinity adenosine A2 receptors decreases the affinity of dopamine D2 receptors in rat striatal membranes. Proc Natl Acad Sci U S A. 1991; 88:7238–7241. [PubMed: 1678519]

Franco R, Canals M, Marcellino D, et al. Regulation of heptaspanning-membrane- receptor function by dimerization and clustering. Trends Biochem Sci. 2003; 28:238–243. [PubMed: 12765835]

Fredholm BB, IJzerman AP, Jacobson KA, Klotz KN, Linden J. International Union of Pharmacology. XXV Nomenclature and classification of adenosine receptors. Pharmacol Rev. 2001; 53:527–552. [PubMed: 11734617]

Fuxe K, Agnati LF, Jacobsen K, et al. Receptor heteromerization in adenosine A2A receptor signaling: relevance for striatal function and Parkinson's disease. Neurology. 2003; 61:S19–23. [PubMed: 14663004]

Gandia J, Galino J, Amaral OB, Soriano A, Lluis C, Franco R, Ciruela F. Detection of higher-order G protein-coupled receptor oligomers by a combined BRET-BiFC technique. FEBS Lett. 2008a; 582:2979–2984. [PubMed: 18675812]

Gandia J, Lluis C, Ferre S, Franco R, Ciruela F. Light resonance energy transfer-based methods in the study of G protein-coupled receptor oligomerization. Bioessays. 2008b; 30:82–89. [PubMed: 18081019]

Gerfen, CR. Basal ganglia, in The Rat Nervous System. Paxinos, G., editor. Elsevier Academic Press; Amsterdam,.: 2004. p. 445-508.

Guo W, Urizar E, Kralikova M, Mobarec JC, Shi L, Filizola M, Javitch JA. Dopamine D2 receptors form higher order oligomers at physiological expression levels. EMBO J. 2008; 27:2293–2304. [PubMed: 18668123]

Hettinger BD, Lee A, Linden J, Rosin DL. Ultrastructural localization of adenosine A2A receptors suggests multiple cellular sites for modulation of GABAergic neurons in rat striatum. J Comp Neurol. 2001; 431:331–346. [PubMed: 11170009]

Jansson A, Goldstein M, Tinner B, Zoli M, Meador-Woodruff JH, Lew JY, Levey AI, Watson S, Agnati LF, Fuxe K. On the distribution patterns of D1, D2, tyrosine hydroxylase and dopamine transporter immunoreactivities in the ventral striatum of the rat. Neuroscience. 1999; 89:473–489. [PubMed: 10077329]

Jordan M, Schallhorn A, Wurm FM. Transfecting mammalian cells: optimization of critical parameters affecting calcium-phosphate precipitate formation. Nucleic Acids Res. 1996; 24:596–601. [PubMed: 8604299]

Kachroo A, Orlando LR, Grandy DK, Chen JF, Young AB, Schwarzschild MA. Interactions between metabotropic glutamate 5 and adenosine A2A receptors in normal and parkinsonian mice. J Neurosci. 2005; 25:10414–10419. [PubMed: 16280580]

Kerppola TK. Complementary methods for studies of protein interactions in living cells. Nat Methods. 2006a; 3:969–971. [PubMed: 17117150]

Kerppola TK. Design and implementation of bimolecular fluorescence complementation (BiFC) assays for the visualization of protein interactions in living cells. Nat Protoc. 2006b; 1:1278–1286. [PubMed: 17406412]

Levey AI, Hersch SM, Rye DB, Sunahara RK, Niznik HB, Kitt CA, Price DL, Maggio R, Brann MR, Ciliax BJ. Localization of D1 and D2 dopamine receptors in brain with subtype-specific antibodies. Proc Natl Acad Sci U S A. 1993; 90:8861–8865. [PubMed: 8415621]

Lindvall O, Bjorklund A. Anatomy of the dopaminergic neuron systems in the rat brain. Adv Biochem Psychopharmacol. 1978; 19:1–23. [PubMed: 358775]

Lopez-Gimenez JF, Canals M, Pediani JD, Milligan G. The alpha1b-adrenoceptor exists as a higher-order oligomer: effective oligomerization is required for receptor maturation, surface delivery, and function. Mol Pharmacol. 2007; 71:1015–1029. [PubMed: 17220353]

Lujan R, Ciruela F. Immunocytochemical localization of metabotropic glutamate receptor type 1 alpha and tubulin in rat brain. Neuroreport. 2001; 12:1285–1291. [PubMed: 11338208]

Milligan G, Bouvier M. Methods to monitor the quaternary structure of G protein- coupled receptors. FEBS J. 2005; 272:2914–2925. [PubMed: 15955052]

Missale C, Nash SR, Robinson SW, Jaber M, Caron MG. Dopamine receptors: from structure to function. Physiol Rev. 1998; 78:189–225. [PubMed: 9457173]

Muller CE, Ferre S. Blocking striatal adenosine A2A receptors: a new strategy for basal ganglia disorders. Recent Patents CNS Drug Discov. 2007; 2:1–21.

Narushima M, Uchigashima M, Hashimoto K, Watanabe M, Kano M. Depolarization-induced suppression of inhibition mediated by endocannabinoids at synapses from fast-spiking interneurons to medium spiny neurons in the striatum. Eur J Neurosci. 2006; 24:2246–2252. [PubMed: 17042791]

Navarro G, Carriba P, Gandia J, Ciruela F, Casado V, Cortes A, Mallol J, Canela EI, Lluis C, Franco R. Detection of heteromers formed by cannabinoid CB1, dopamine D2, and adenosine A2A G-protein-coupled receptors by combining bimolecular fluorescence complementation and bioluminescence energy transfer. ScientificWorldJournal. 2008; 8:1088–1097. [PubMed: 18956124]

Obeso JA, Rodriguez-Oroz MC, Rodriguez M, Lanciego JL, Artieda J, Gonzalo N, Olanow CW. Pathophysiology of the basal ganglia in Parkinson's disease. Trends Neurosci. 2000; 23:S8–19. [PubMed: 11052215]

Ossowska K, Konieczny J, Wolfarth S, Wieronska J, Pilc A. Blockade of the metabotropic glutamate receptor subtype 5 (mGluR5) produces antiparkinsonian-like effects in rats. Neuropharmacology. 2001; 41:413–420. [PubMed: 11543761]

Paquet M, Smith Y. Group I metabotropic glutamate receptors in the monkey striatum: subsynaptic association with glutamatergic and dopaminergic afferents. J Neurosci. 2003; 23:7659–7669. [PubMed: 12930805]

Popoli P, Pezzola A, Torvinen M, Reggio R, Pintor A, Scarchilli L, Fuxe K, Ferre S. The selective mGlu(5) receptor agonist CHPG inhibits quinpirole-induced turning in 6-hydroxydopamine-lesioned rats and modulates the binding characteristics of dopamine D(2) receptors in the rat striatum: interactions with adenosine A(2a) receptors. Neuropsychopharmacology. 2001; 25:505–513. [PubMed: 11557164]

Rodrigues RJ, Alfaro TM, Rebola N, Oliveira CR, Cunha RA. Co-localization and functional interaction between adenosine A(2A) and metabotropic group 5 receptors in glutamatergic nerve terminals of the rat striatum. J Neurochem. 2005; 92:433–441. [PubMed: 15659214]

Rosin DL, Robeva A, Woodard RL, Guyenet PG, Linden J. Immunohistochemical localization of adenosine A2A receptors in the rat central nervous system. J Comp Neurol. 1998; 401:163–186. [PubMed: 9822147]

Sarrio S, Casado V, Escriche M, Ciruela F, Mallol J, Canela EI, Lluis C, Franco R. The heat shock cognate protein hsc73 assembles with A(1) adenosine receptors to form functional modules in the cell membrane. Mol Cell Biol. 2000; 20:5164–5174. [PubMed: 10866672]

Schiffmann SN, Fisone G, Moresco R, Cunha RA, Ferre S. Adenosine A2A receptors and basal ganglia physiology. Prog Neurobiol. 2007; 83:277–292. [PubMed: 17646043]

Schiffmann SN, Jacobs O, Vanderhaeghen JJ. Striatal restricted adenosine A2 receptor (RDC8) is expressed by enkephalin but not by substance P neurons: an in situ hybridization histochemistry study. J Neurochem. 1991; 57:1062–1067. [PubMed: 1713612]

Schmidt U, Richter K, Berger AB, Lichter P. In vivo BiFC analysis of Y14 and NXF1 mRNA export complexes: preferential localization within and around SC35 domains. J Cell Biol. 2006; 172:373–381. [PubMed: 16431928]

Tozzi A, Tscherter A, Belcastro V, Tantucci M, Costa C, Picconi B, Centonze D, Calabresi P, Borsini F. Interaction of A2A adenosine and D2 dopamine receptors modulates corticostriatal glutamatergic transmission. Neuropharmacology. 2007; 53:783–789. [PubMed: 17889039]

Uchigashima M, Narushima M, Fukaya M, Katona I, Kano M, Watanabe M. Subcellular arrangement of molecules for 2-arachidonoyl-glycerol-mediated retrograde signaling and its physiological contribution to synaptic modulation in the striatum. J Neurosci. 2007a; 27:3663–3676. [PubMed: 17409230]

Uchigashima M, Narushima M, Fukaya M, Katona I, Kano M, Watanabe M. Subcellular arrangement of molecules for 2-arachidonoyl-glycerol-mediated retrograde signaling and its physiological contribution to synaptic modulation in the striatum. J Neurosci. 2007b; 27:3663–3676. [PubMed: 17409230]

Vidi PA, Chen J, Irudayaraj JM, Watts VJ. Adenosine A(2A) receptors assemble into higher-order oligomers at the plasma membrane. FEBS Lett. 2008; 582:3985–3990. [PubMed: 19013155]

Xia Y, Yu H, Jansen R, Seringhaus M, Baxter S, Greenbaum D, Zhao H, Gerstein M. Analyzing cellular biochemistry in terms of molecular networks. Annu Rev Biochem. 2004; 73:1051–1087. [PubMed: 15189167]

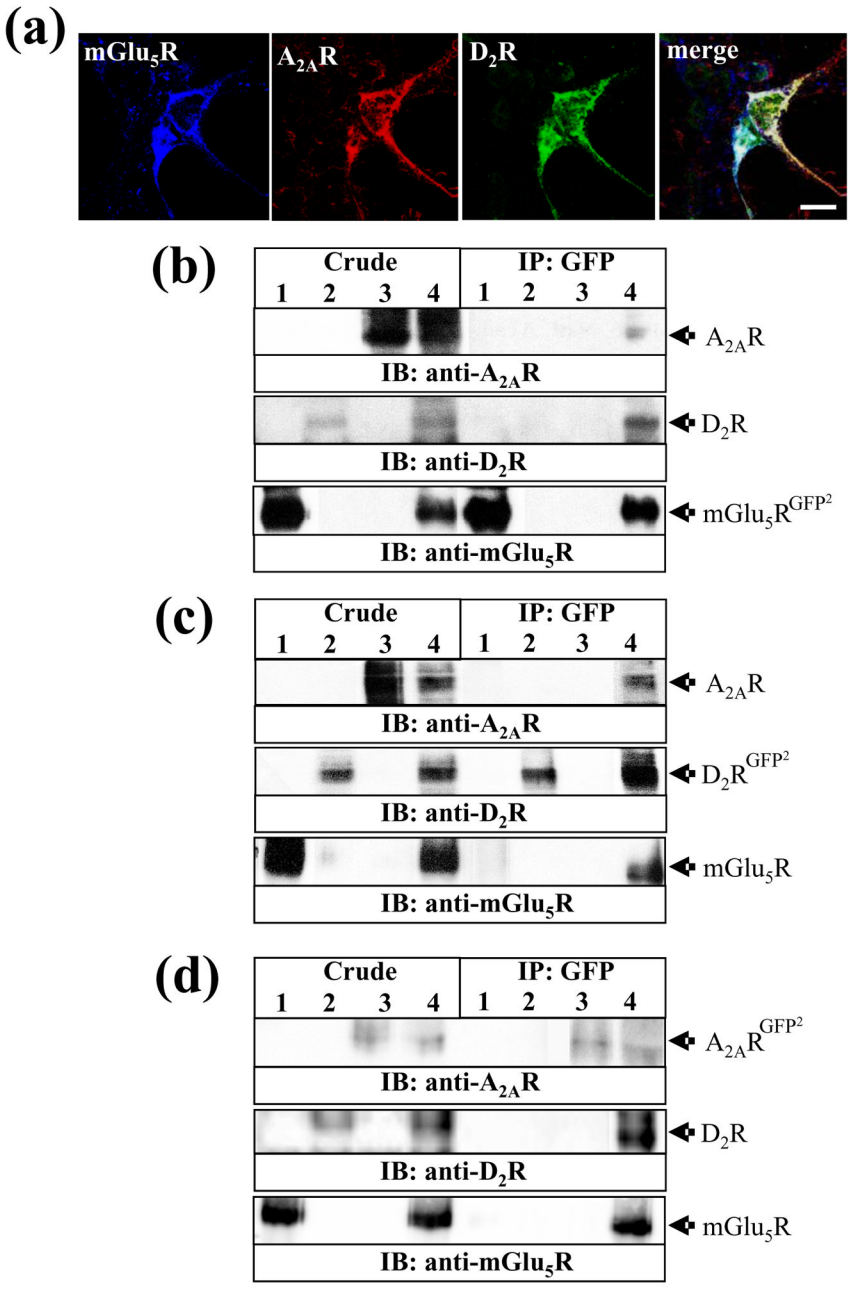

Fig. 1.

Heteromerization in HEK cells. Immunofluorescence localization of $mGlu_5R$, $A_{2A}R$ and D_2R in transiently transfected HEK-293 cells (panel a). Cells were transiently cotransfected with the cDNA's encoding $mGlu_5R$, $A_{2A}R$ and D_2R and processed for immunostaining (see Materials and methods) using a rabbit anti-$mGlu_5R$, a mouse anti-$A_{2A}R$ and a goat anti-D_2R. The bound primary antibody was detected using donkey-anti-rabbit-Cy5 (1/500), donkey-anti-mouse-Cy3 (1/500) and donkey-anti-goat-Cy2 (1/500). Superimposition of images reveals a high receptor codistribution in white (merge). Scale bar: 10 μm. Coimmunoprecipitation assays in HEK-293 cells (panels b, c and d). (b) Cells were transiently transfected with $mGlu_5R^{GFP2}$ (lane 1), D_2R (lane 2), $A_{2A}R$ (lane 3) or with all three receptors simultaneously (lane 4). (c) Cells were transiently transfected with $mGlu_5R$

(lane 1), D_2R^{GFP2} (lane 2), $A_{2A}R$ (lane 3) or with all three receptors simultaneously (lane 4). (d) Cells were transiently transfected with $mGlu_5R$ (lane 1), D_2R (lane 2), $A_{2A}R^{GFP2}$ (lane 3) or with all three receptors simultaneously (lane 4). Cells were washed, solubilized and processed for immunoprecipitation using anti-GFP monoclonal antibody (2 μg/ml; IP: GFP). Solubilized membranes (Crude; 20 μg) and immunoprecipitates (IP) were analyzed by SDS-PAGE and immunoblotted using rabbit anti-$A_{2A}R$ whole serum (1/2000), rabbit anti-D_2R whole serum (1/2000) or rabbit anti-$mGlu_5R$ polyclonal antibody (1 μg/ml) and horseradish-peroxidase (HRP)-conjugated goat anti-rabbit IgG as a secondary antibody. These blots are representative of four different experiments with similar qualitative results.

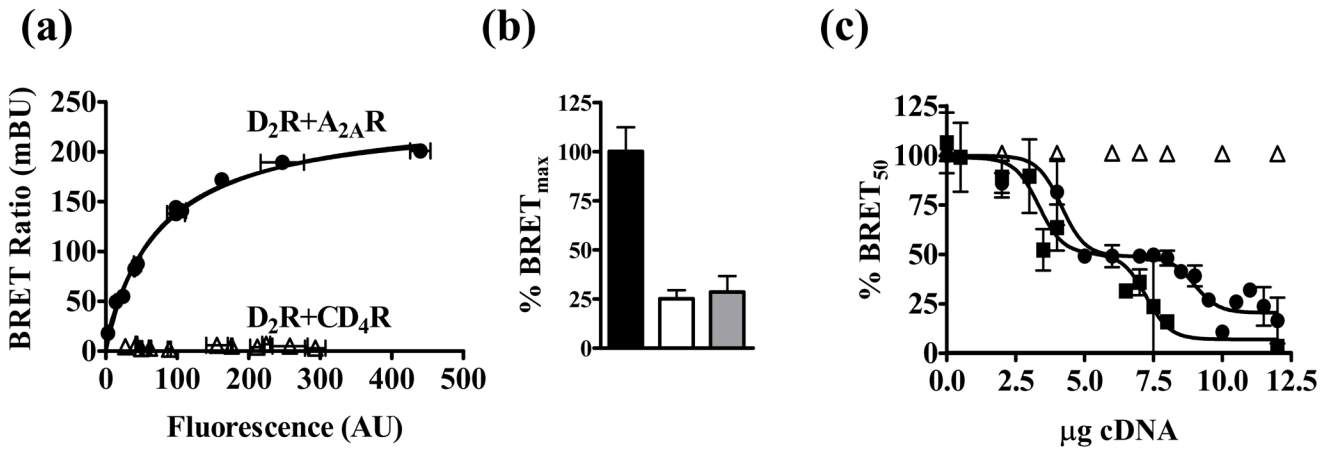

Fig. 2.

BRET-based study of receptor heteromerization in HEK-293 cells. BRET saturation experiments between D_2R^{Rluc} and $A_{2A}R^{YFP}$ (●) or D_2R^{Rluc} and CD_4R^{YFP} (△) (panel a). Both fluorescence and luminescence of each sample were measured prior to every experiment to confirm equal expression of *R*luc construct while monitoring the increase of YFP expression. mBU is the BRET ratio x1000 (see Materials and methods). Error bars indicate SD of mean specific BRET ratio (mBU) values of five individual experiments grouped as a function of the amount of fluorescence of the acceptor. (b) Comparison of the $BRET_{max}$ obtained for $D_2R^{Rluc}/A_{2A}R^{YFP}$ (solid bar), D_2R^{Rluc}/A_1R^{YFP} (white bar) and $D_2R^{Rluc}/GABA_{B2}R^{YFP}$ (grey bar) under similar experimental conditions. Results are expressed as a percentage of the $BRET_{max}$ obtained for the $D_2R^{Rluc}/A_{2A}R^{YFP}$ pair. (c) Displacement study of a constant BRET ratio (~$BRET_{50}$) of $A_{2A}R^{Rluc}/D_2R^{YFP}$ pair by increasing amounts of $mGlu_5R$ (●) or CD_4R (△) constructs. Also, a constant BRET ratio (~$BRET_{50}$) of $D_2R^{Rluc}/mGlu_5R^{YFP}$ pair was displaced by increasing amounts of $A_{2A}R$ (■).

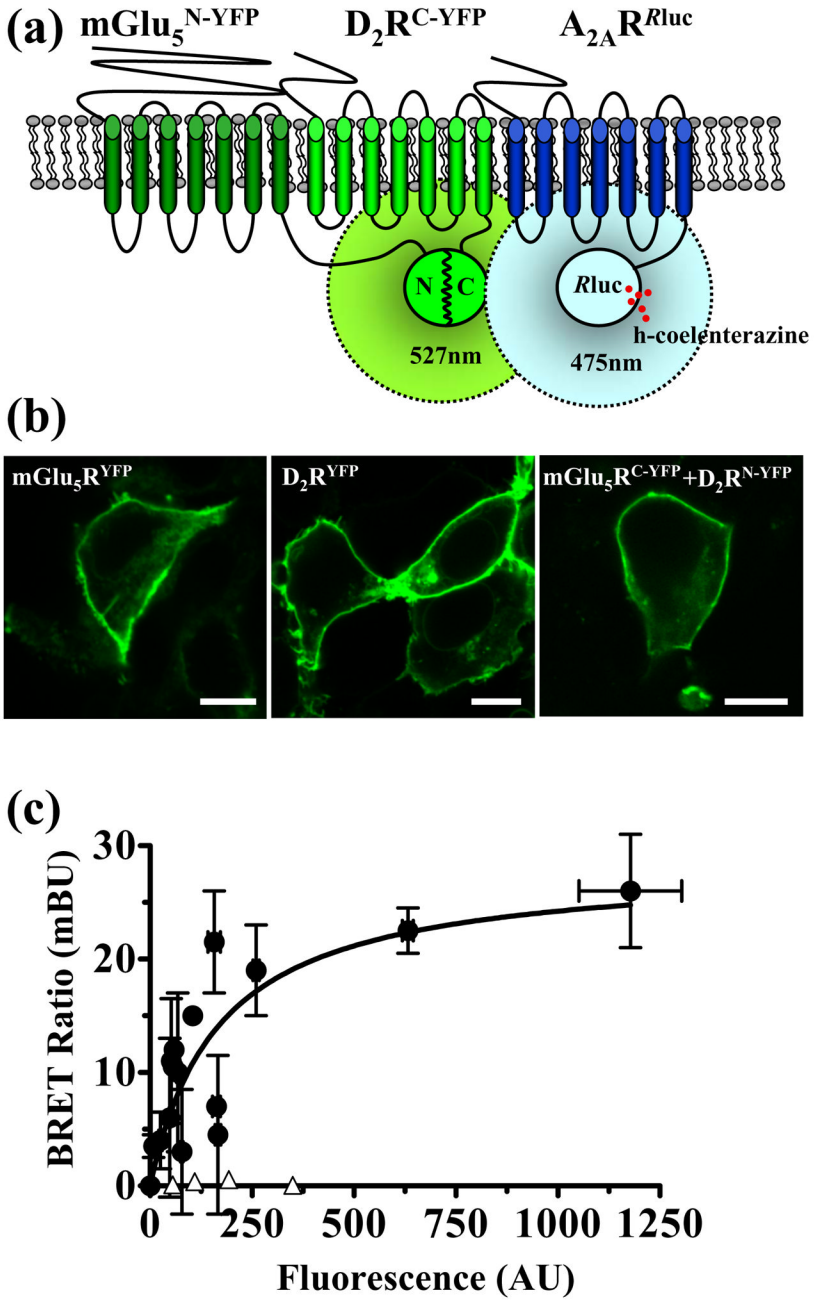

Fig. 3.

Detection of $mGlu_5R/A_{2A}R/D_2R$ heteromeric complexes by combined BRET/BiFC assays. (a) Schematic representation of the combined BRET/BiFC assay. BRET signal is triggered by the oxidation of h-coelenterazine by the *R*luc fused to the C-terminal tail of the $A_{2A}R^{Rluc}$ construct. This enzymatic reaction produces light emission at 475 nm, which might excite a proper fluorophore acceptor found in close proximity (within 10 nm). As acceptor we use the $mGlu_5R/D_2R$ heterodimer-mediated complemented-YFP ($mGlu_5R^{N\text{-}YFP}/D_2R^{C\text{-}YFP}$) that after excitation it emits at 527 nm. (b) Visualization of $mGlu_5R/D_2R$ heterodimer by BiFC assays. HEK cells were transiently transfected with 5 μg of the cDNA encoding $mGlu_5R^{YFP}$, D_2R^{YFP} or $mGlu_5R^{N\text{-}YFP}$ (5 μg) plus $D_2R^{C\text{-}YFP}$ (5 μg) and processed for

confocal microscopy imaging. Microscope observations were made with Olympus Fluoview 500 confocal scanning laser adapted to an inverted Olympus IX-70 microscope. Scale bar: 10 μm. (c) BRET saturation curve. BRET was measured in HEK cells coexpressing $A_{2A}R^{Rluc}$ and $mGlu_5R^{N\text{-}YFP}+D_2R^{C\text{-}YFP}$ (●) or $A_{2A}R^{Rluc}$ and $GABA_{B2}R^{YFP}$ (△) constructs. Co-transfections were performed with increasing amounts of plasmid DNA for the YFP construct whereas the DNA for the *R*luc construct was maintained constant. Both fluorescence and luminescence of each sample were measured prior to every experiment to confirm equal expression of *R*luc while monitoring the increase of YFP expression (see Materials and methods).

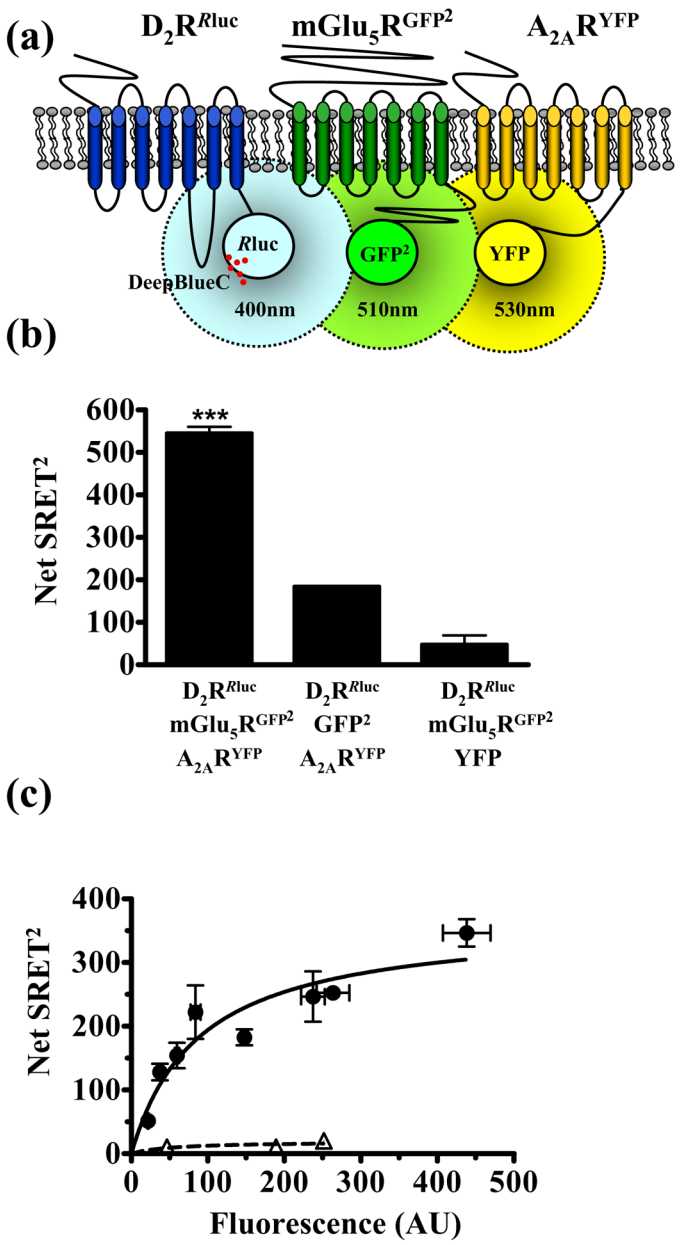

Fig. 4.

Detection of $mGlu_5R/A_{2A}R/D_2R$ heteromeric complexes by SRET assays. Schematic representation of the SRET assay (panel a). The initial BRET signal is triggered by the oxidation of DeepBlueC by the *R*luc fused to the C-terminal tail of the D_2R^{Rluc} construct. This enzymatic reaction produces light emission at 400 nm, which might excite a proper fluorophore acceptor, for instance $mGlu_5R^{GFP2}$, if found in close proximity (within 10 nm). This fluorophore acceptor ($mGlu_5R^{GFP2}$)can engage now in a FRET process acting as a donor whose emission light at 510 nm can excite a suitable acceptor ($A_{2A}R^{YFP}$), thus ending in a net 530 nm fluorescence emission. (b) NetSRET was measured in HEK-293 cells co-expressing D_2R^{Rluc}, $mGlu_5R^{GFP2}$ and $A_{2A}R^{YFP}$. Fluorescence and luminescence of each sample were measured prior to every experiment to confirm similar expression levels. Data, expressed as net SRET are means ± SEM of three independent experiments performed in

triplicate. One-way ANOVA followed by Newman-Keuls test showed significant differences respect to both negative controls. ***$p<0.001$. (c) SRET saturation was measured in HEK-293 cells co-expressing D_2R^{Rluc}, $mGlu_5R^{GFP2}$ (in a constant ratio 2 μg and 4 μg, respectively) with increasing amounts of the $A_{2A}R^{YFP}$ (●) or CD_4R^{YFP} (△). Net SRET was detected for $D_{2L}R^{Rluc}/mGlu_5R^{GFP2}/A_{2A}R^{YFP}$ compared with net SRET detected with cells expressing only $D_{2L}R^{Rluc}$ plus $mGlu_5R^{GFP2}$.

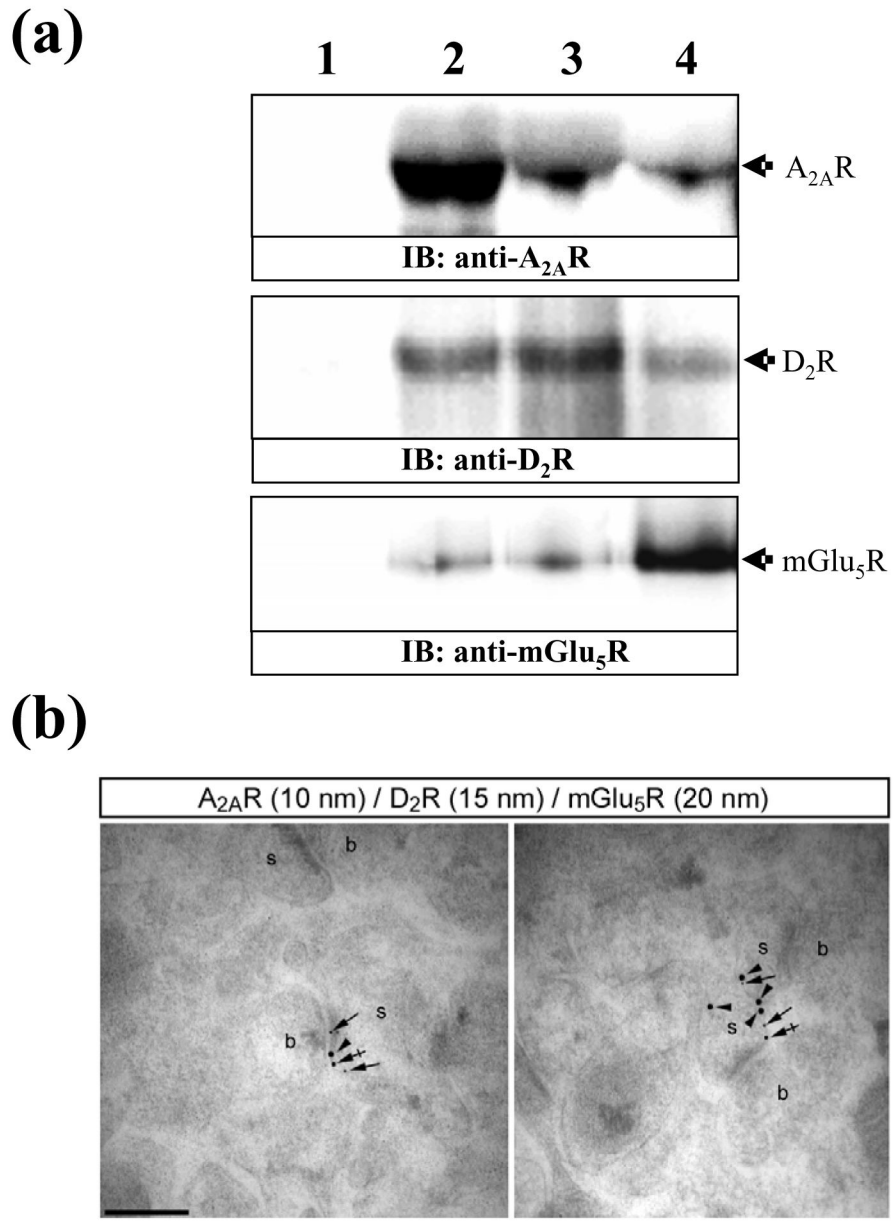

Fig. 5.

Interaction of $A_{2A}R$, D_2R and $mGlu_5R$ in rat striatum. (a) Co-immunoprecipitation of $A_{2A}R$, D_2R and $mGlu_5R$ from rat striatum. Rat striatal membanes were solubilized and processed for immunoprecipitation using control rabbit IgG (5μg/ml; lane 1), rabbit anti-$A_{2A}R$ polyclonal antibody (5μg/ml; lane 2), rabbit anti-D_2R polyclonal antibody (5μg/ml; lane 3) and rabbit anti-$mGlu_5R$ polyclonal antibody (5μg/ml; lane 4). Immunoprecipitates were analyzed by SDS-PAGE and immunoblotted using rabbit anti-$A_{2A}R$ whole serum (1/2000), rabbit anti-D_2R whole serum (1/2000) or rabbit anti-$mGlu_5R$ polyclonal antibody (1 μg/ml) and HRP-conjugated anti-rabbit IgG TrueBlot™ (1/1000) as a secondary antibody. These blots are representative of three different experiments with similar qualitative results. (b) Subcellular distribution of $A_{2A}R$, D_2R and $mGlu_5R$ in rat striatum. Electron micrographs showing immunoreactivity for $A_{2A}R$, D_2R and $mGlu_5R$ in rat striatum as revealed using a

triple-labelling post-embedding immunogold technique. Immunoparticles for $A_{2A}R$ (10 nm size, arrows), D_2R (15 nm size, crossed arrows) and $mGlu_5R$ (20 nm size, arrowheads) were detected along the extrasynaptic and perisynaptic plasma membrane of the same dendritic spine (s) establishing excitatory synaptic contact with axon etrminals (b). Scale bar: 0.2 μm.